# Journal of Materials Chemistry A

Accepted Manuscript






ROYAL SOCIETY OF CHEMISTRY

www.rsc.org/materialsA

# Spinneret as the key component for surface-porous graphene fibers in high energy density micro-supercapacitors

Weihua Cai, Ting Lai and Jianshan Ye *

College of Chemistry and Chemical Engineering, South China University of Technology, Guangzhou 510641, P. R. China.

* Corresponding author. Tel: +86-20-87113241, Fax: +86-20-87112901, E-mail: jsye@scut.edu.cn

**Abstract**

A metal needle spinneret was found to be the key component to synthesize neat graphene fibers with porous surface in the wet spinning process. Flexible solid-state micro-supercapacitors (micro-SCs) based on the neat graphene fibers was then designed and fabricated. The as-prepared graphene fibers with an impressive specific surface areas up to 839 $m^2 \cdot g^{-1}$ achieved an excellent specific capacitance of 228 $mF \cdot cm^{-2}$ at 39.7 $\mu A \cdot cm^{-2}$. The assembled micro-SCs exhibit excellent performance such as high energy densities of 7.9 $\mu Wh \cdot cm^{-2}$ (or 4.0 $mWh \cdot cm^{-3}$) approaching those of lithium thin film batteries and excellent long life stability. This research opens the door to synthesize surface-porous neat graphene fibers and these fibers are promising as electrode materials in high-performance micro-SCs.

**Keywords:** Flexible electrochemical capacitors; Solid-state micro-supercapacitors; Neat graphene fibers; Nanoscale porous surface; Spinnerets.

# 1. Introduction

With the wide use of wearable and portable electronics in our daily life, the miniaturization of energy storage devices has become an urgent challenge. [1-4] The micro-supercapacitors (micro-SCs) are one of the most promising energy storage devices since that they can offer high power densities, much longer lifetimes and faster charge/discharge rates. [5-7] However, the key problem for the practical application of micro-SCs is to increase the energy density without sacrificing the other electrochemical properties such as device power density and cycle life. [8-10] Though considerable efforts have been made on carbon based micro-SCs including graphene fibers or carbon nanotube (CNT) fibers based micro-SCs [11, 12] such as graphene/$MnO_2$ fibers[13], graphene/$Bi_2O_3$ fibers[14], graphene/CNT fibers[12], CNT/mesoporous carbon fibers[15], CNT/$MnO_2$ fibers[16] and CNT/graphene nitrogen doped fibers[17], the neat graphene fibers used as substrates in most of the previous reports hardly show satisfactory electrochemical performance in supercapacitors. It is still a critical challenge to essentially improve the specific capacitance of the neat graphene fibers. One reason for the relatively low specific capacitance of the neat fibers may be attributed to the less ion accessible surface area. In one case reported by Meng et al., the all-graphene core-sheath fibers were fabricated and assembled into fiber-shaped micro-SCs. But their devices could only achieve the maximum areal specific capacitance of 1.7 $mF \cdot cm^{-2}$ with poor energy density of 0.17$\mu Wh \cdot cm^{-2}$. [18] So far, there are very few reports that focus on enhancing the energy density of neat graphene fibers. To synthesize the neat graphene fibers with highly porous surface is

still an obstacle on the way to make high energy density micro-SCs.

Herein, a metal needle from a medical syringe as the spinneret was found to be efficient to synthesize neat graphene fibers containing nanoscale surface-porous sheets with specific surface area up to 839 $m^2 \cdot g^{-1}$ (denoted as SGFs). The SGFs were assembled into flexible solid-state micro-SCs. These fibers showed an impressive areal specific capacitance as high as 228 $mF \cdot cm^{-2}$ at 39.7 $\mu A \cdot cm^{-2}$ in a two-electrode cell , which is almost 2 orders of magnitude higher than that of the previous HI solutions treated graphene fibers synthesized by Chao Gao group who applied a glass syringe as the spinneret (3.3 $mF \cdot cm^{-2}$).[19] Our micro-SCs assembled with the SGFs display remarkable energy densities up to 4.0 $mWh \cdot cm^{-3}$, which are comparable to those of thin-film lithium batteries. For comparison, the neat graphene fibers were also produced by using a polytetrafluoroethylene (PTFE) tube as the spinneret (denoted as PGFs, Figure S1 in Supporting Information). However, these PGFs displayed much less specific capacitance (47.2 $mF \cdot cm^{-2}$) than that of the SGFs.

## 2. Experimental section

**Preparation of GO gel solutions**

GO was synthesized from natural flake graphite by a modified Hummers method without sonication as the previous report. [20] After the centrifugation at 10000 rpm for 15 minutes, we obtained the GO gel solution at the bottom of a centrifugal tube. The gel solutions of GO were about 5 $mg \cdot ml^{-1}$.

**Preparation of fiber electrodes**

A metal needle from a medical syringe instead of a glass spinneret was adopted as the

spinneret for the wet spinning SGOFs. For comparison, a PTFE tube was also used as the spinneret to prepare PGOFs. During the spinning process for SGOFs and PGOFs, the GO gel solutions were injected into the ethanol/water (1:3 v/v) solution of 5 wt% NaOH under 1.5 MPa held by $N_2$. The as-prepared SGOFs or PGOFs were rolled onto a drum, washed by ethanol for several times and dried under room temperature. The SGFs (or PGFs) were obtained by chemical reduction of SGOFs (or PGOFs) in aqueous solution of HI (40%) at 80℃for 6 hours.

**Fabrication of fiber micro-SC**

PVA-$H_2SO_4$ gel was used as a solid electrolyte. PVA-$H_2SO_4$ electrolyte was simply made as follows: 1.0 g $H_2SO_4$ was mixed with 10 mL DI water and then 1.0 g PVA powder was added. The whole mixture was heated to 85 °C under vigorously stirring until the solution became clear. Two parallel SGFs' (or PGFs') electrodes were mounted onto a PET substrate using the PVA-$H_2SO_4$ electrolyte and their position was adjusted by an optical microscope. Finally, the assemble micro-SC was dried under ambient conditions until the PVA- $H_2SO_4$ gel solidified.

**Characterization and instrumentation**

The SEM images were recorded on Hitachi S-3700 with an accelerating voltage of 10.0 kV or 20.0 kV. Atomic force microscopy (AFM) was conducted on PARK, XE-100. Brunauere-Emmette-Teller (BET, BeiShiDe Instrument, 3H-2000PS1) specific surface area was obtained from the $N_2$ adsorption/desorption isotherm recorded at 77 K. X-ray diffraction (XRD) patterns were collected from a Bruker AXS D8-Advanced diffractometer with Cu Kα radiation (λ =1.5418 Å). Raman

spectra were taken on LabRAM Aramis (HJY, France). All electrochemical measurements were performed on a CHI660E electrochemical workstation (Chenhua, China). Tensile strength tests were conducted with an Instron material testing system (Instron 3367). UV-visible spectroscopy was conducted on Hitachi U-3900H.

## 3. Results and discussion

Figure 1 shows the processing steps of this work. An apparatus was built to synthesize the syringe's metal needle based GO fibers (SGOFs). We selectively adopt a metal needle as the spinneret which is the key component to produce surface-porous neat graphene fibers. The continuous wet spinning SGOFs could be obtained by injecting the graphene oxide (GO) gel solutions into the coagulation bath that is ethanol/water (1:3 v/v) solution of 5 wt% NaOH (Figure 2a). The as-prepared SGOFs could be treated by diluted HI solutions at 80 ℃ for 6 hours to obtain SGFs. After the further treatment, the wet or dry flexible but tough SGFs could be bent into different shapes (Figure 2b). Due to the high conductivity of SGFs (567 $S \cdot cm^{-1}$) which is 7 orders of magnitude higher than that of SGOFs ($2.27 \times 10^{-5}$ $S \cdot cm^{-1}$) (Figure 2d, calculated methods in Figure S1), the SGFs had been also applied as effective conducting wires (Figure 2c). Two SGFs were used as conducting wires to connect a blue light emission dioxide (LED) with a power supply. The as-prepared dry SGFs also exhibit good tensile strength (about 140 MPa, Figure S2), which is comparable to those of the previous reports. [21, 22]

To figure out the difference between the as-prepared SGFs and PGFs, the surface inside the spinnerets and the responding fibers were characterized by scanning

electron microscope (SEM), respectively in Figure 3. When compared with the smooth surface inside the PTFE tube (Figure 3g, h), the inwall of metal needle (Figure 3a-c) appeared to be rough. The exterior roughness of the two different surfaces was characterized by 3 Dimensional Surface Profilometer. The roughness of the surface inside the metal needle was calculated to be 0.94 μm, which was 2 times larger than that (0.48 μm) of PTFE tube (Figure S3). In the case of SGFs (Figure 3d-f), a rather rough texture of the fibers could be clearly seen. Along the fiber's main axis, SGFs have been shrunk during the drying process while the surface of SGFs still maintains nanoscale porous structure with flowers-like sheets which may lead to high accessible surface area for the ions in the electrolyte. Such unique formation of the SGFs is resulted from the concave-convex shaped inwall of the needle of the syringe (Figure 3c). In contrast, the PGFs possess a rather smooth lengthways outwall (Figure 3i) probably because of the glossy inwall of the PTFE tube (Figure 3g, h). As a result, the SGFs achieve a specific surface area of 839 $m^2 \cdot g^{-1}$ which was much higher than that of PGFs (49 $m^2 \cdot g^{-1}$) (MB adsorption method in the Supporting Information) and those of reported carbon based fibers including RGO fibers (18 $m^2 \cdot g^{-1}$)[23], carbon microfibers (<10 $m^2 \cdot g^{-1}$)[24], wet-spun SWNT fibers (160 $m^2 \cdot g^{-1}$)[25]. The BET results also confirmed that the specific surface area of SGFs (815 $m^2 \cdot g^{-1}$) was much larger than that of PGFs (42 $m^2 \cdot g^{-1}$, Figure S7). These results may indicate that our SGFs have great potentials for high performance micro-SCs. Besides, the XRD and Raman spectrum show no obvious difference in the interior structure between the SGFs and PGFs (Figure S8).

The two-electrode system was used to test the assembled micro-SCs based on SGFs to explore the advantages of these flexible electrochemical capacitors for the real application. Typically, two parallel SGFs were mounted onto a flexible polyester (PET) substrate using polyvinyl alcohol (PVA)-$H_2SO_4$ electrolyte without binders, separators or any other packaging materials (see experimental section for a detailed description). Figure 4a displays the cyclic voltammetry (CV) curves of micro-SCs which are based on SGFs (red curve) and PGFs (black curve), respectively. As seen from Figure 4a, the current density of the micro-SC based on SGFs are nearly 2 times larger than that of the micro-SC based on PGFs. An almost rectangular shape within 0-1V could be obtained in the CV curves of the micro-SCs based on SGFs at various scanning rates from 2 $mV \cdot s^{-1}$ to 10 $mV \cdot s^{-1}$ (Figure 4b). Moreover, its galvanostatic charge/discharge (CC) curves (Figure 4c) at various current densities were also recorded to further evaluate the performance of the flexible device based on the SGFs. These charge curves are relatively symmetric to their corresponding discharge counterparts at the current densities from 0.12 $mA \cdot cm^{-2}$ to 0.32 $mA \cdot cm^{-2}$, further revealing the good capacitive behavior of the flexible all-solid-state micro-SCs. The specific volumetric capacitance of a single SGFs' electrode was calculated to be 228 $mF \cdot cm^{-2}$ at 39.7 $\mu A \cdot cm^{-2}$, the highest value to date among the micro-SCs tested by two-electrode system (Figure 4d) [13-18, 26-36] (details listed in Table S1 in Supporting Information). Since there were no obvious differences in the interior structure between the SGF and PGF as mentioned above, the high specific capacitance of SGF was attributed to the high specific area of SGF (839 $m^2 \cdot g^{-1}$ by the MB method, 815

$m^2 \cdot g^{-1}$ by the BET method). Because the roughness of the inwall is the only difference between the metal needle and the PTFE tube, the origin of the high specific area of SGF was the rough inwall of the metal needle spinneret which was the graphene fiber going through.

Figure 5a shows that the micro-SCs based on the SGFs still retain 98.5% of the initial capacitances after 10000 charge/discharge cycles, demonstrating its impressive cycling stability with a long cycle life. The inset of Figure 5a shows the corresponding micro-SCs were charged and discharged for 7 cycles after 10000 cycles. These results indicate our micro-SCs may have promising perspectives in the real applications. Our flexible all-solid-state micro-SCs also show excellent mechanical robustness in the bending test. The CV performance of this device under different conditions is shown in Figure 5b (the inset is the corresponding digital image at the bending condition). There are no significant differences as the device was bent after 100 times, indicating that the changes of the electrochemical performance are negligible under bending condition. The areal or volumetric energy/power densities of a micro-SC are more meaningful properties while evaluating a micro-device than the gravimetric energy/power densities [37]. Figure 5c-d displays Ragone plots (power density *vs* energy density) to compare our SGFs based devices with the previously reported solid-state supercapacitors. Note that, the power density and energy density shown are based on two SGFs' electrodes, excluding electrolyte. Figure 5c shows the areal Ragone plots and the corresponding volumetric Ragone plots are also exhibited in Figure 5d. The areal energy density varied from 7.9 $\mu Wh \cdot cm^{-2}$ to 5.3 $\mu Wh \cdot cm^{-2}$ in

the power density range of 19.8 $\mu W \cdot cm^{-2}$ to 1047.9 $\mu W \cdot cm^{-2}$ for the micro-SCs based on SGFs, whose areal energy density is about 40 times higher than that of the all-graphene core-sheath fiber supercapacitors. [18] As for the micro-SCs based on SGFs, the volumetric energy densities varied from 4.0 $mWh \cdot cm^{-3}$ to 1.5 $mWh \cdot cm^{-3}$ in the power densities range of 10.0 $mW \cdot cm^{-3}$ to 301.6 $mW \cdot cm^{-3}$. This volumetric energy density is also higher than that of the recently reported thin-film supercapacitors based on laser-scribed graphene (about 1.4 $mWh \cdot cm^{-3}$ in ionic liquid) [9] and is about 10 times higher than the commercial available supercapacitors (5.5 V/100 mF) [17]. Besides, the volumetric power density of the micro-SCs based on SGFs is more than one order of magnitude higher than that of lithium thin film batteries. [1] As far as we know, the electrochemical performances of our micro-SCs based on SGFs are remarkable among the best works reported to date (details listed in Table S1 in Supporting Information).

To verify the potential usefulness of these neat graphene fibers with nanoscale porous surface, we have connected three micro-SCs units (based on SGFs) in series or in parallel to make a device. The three micro-SCs connected in series exhibit a 3 V charge/discharge voltage with similar discharge time when they are compared with a single micro-SC with an operating voltage of 1.0 V (Figure 6a-b). Moreover, the discharge time of the three parallel micro-SCs is three times than that of a single micro-SC when operated at the same current density (Figure 6c-d). Figure 6e-f also further confirms the potential application of the micro-SCs based on SGFs as efficient energy storage components for wearable or flexible electronic devices. The device

(two micro-SCs in parallel and then further connected with another micro-SC in series) could be charged up to 1.53 V by a commercial flexible solar cell under a 500 W lamp (a video shown in Supporting Information).

## 4. Conclusion

In summary, we have creatively developed an efficient method to continuously produce neat graphene fibers with nanoscale porous surface by employing a metal needle from a medical syringe as the spinneret during wet spinning. Our investigation reveals that the as-prepared neat graphene fibers achieve so much high specific areal surfaces up to 839 $m^2 \cdot g^{-1}$. Upon on the proof-of-concept study, we have shown that the neat SGFs possesses a specific volumetric capacitance up to 228 $mF \cdot cm^{-2}$ at 39.7 $\mu A \cdot cm^{-2}$ in a two-electrode cell. Besides, the micro-SCs based on SGFs exhibit long life cycle stability (98.7% device capacitance retention over 5000 cycles), remarkable areal energy density (7.9 $\mu Wh \cdot cm^{-2}$) and impressive volumetric energy density (4.0 $mWh \cdot cm^{-3}$) which is comparable to that of thin-film lithium batteries. Our micro-SCs based device could be charged by a commercially flexible solar cell up to 1.53 V and are potential in wearable and flexible electronic devices.

## Acknowledgment

The authors gratefully acknowledge the financial support by NSFC (21372088).

# References

[1] D. Pech, M. Brunet, H. Durou, P. Huang, V. Mochalin, Y. Gogotsi, P.L. Taberna, P. Simon. *Nat. Nanotechnol.* 2010, 5, 651-654.

[2] W. Gao, N. Singh, L. Song, Z. Liu, A. L. M. Reddy, L. Ci, R. Vajtai, Q. Zhang, B. Wei, P. M. Ajayan. *Nat. Nanotechnol.* 2011, 6, 496-500.

[3] M. F. El-Kady, R. B. Kaner. *Nat. Commun.* 2013, 4.DOI: 10.1038/ncomms2446

[4] Q. Meng, H. Wu, Y. Meng, K. Xie, Z. Wei, Z. Guo. *Adv. Mater.* 2014, 26, 4100-4106.

[5] J. Chmiola, C. Largeot, P.-L. Taberna, P. Simon, Y. Gogotsi. *Science* 2010, 328, 480-483.

[6] X. Wang, B. Liu, R. Liu, Q. Wang, X. Hou, D. Chen, R. Wang, G. Shen. *Angew. Chem.Int. Ed.* 2014, 53, 1849-1853.

[7] L. Kou, T. Huang, B. Zheng, Y. Han, X. Zhao, K. Gopalsamy, H. Sun, C. Gao. *Nat. Commun.* 2014, 5.DOI: 10.1038/ncomms4754

[8] S. H. Aboutalebi, R. Jalili, D. Esrafilzadeh, M. Salari, Z. Gholamvand, S. A. Yamini, K. Konstantinov, R. L. Shepherd, J. Chen, S. E. Moulton *et al. ACS Nano* 2014, 8, 2456-2466.

[9] M. F. El-Kady, V. Strong, S. Dubin, R. B. Kaner. *Science* 2012, 335, 1326-1330.

[10] Y. Xu, Z. Lin, X. Zhong, X. Huang, N. O. Weiss, Y. Huang, X. Duan. *Nat. Commun.* 2014, 5. DOI: 10.1038/ncomms5554

[11] T. Chen, L. Dai. *J. Mater. Chem. A* 2014, 2, 10756-10775.

[12] H. Sun, X. You, J. Deng, X. Chen, Z. Yang, J. Ren, H. Peng. *Adv. Mater.* 2014, 26, 2868-2873.

[13] C. Qing, M. Yuning, H. Chuangang, Z. Yang, S. Huibo, C. Nan, Q. Liangti. *J. Power Sources* 2014, 247, 32-39.

[14] K. Gopalsamy, Z. Xu, B. Zheng, T. Huang, L. Kou, X. Zhao, C. Gao. *Nanoscale* 2014, 6, 8595-8600.

[15] J. Ren, W. Bai, G. Guan, Y. Zhang, H. Peng. *Adv. Mater.* 2013, 25, 5965-5970.

[16] J. Ren, L. Li, C. Chen, X. Chen, Z. Cai, L. Qiu, Y. Wang, X. Zhu, H. Peng. *Adv. Mater.* 2013, 25, 1155-1159.

[17] D. Yu, K. Goh, H. Wang, L. Wei, W. Jiang, Q. Zhang, L. Dai, Y. Chen. *Nat. Nanotechnol.* 2014, 9, 555-562.

[18] Y. Meng, Y. Zhao, C. Hu, H. Cheng, Y. Hu, Z. Zhang, G. Shi, L. Qu. *Adv. Mater.* 2013, 25, 2326-2331.

[19] T. Huang, B. Zheng, L. Kou, K. Gopalsamy, Z. Xu,C. Gao, Y. Meng and Z. Wei. *RSC Adv.* 2013, 3, 23957-23962.

[20] Z. Xu, C. Gao. Graphene chiral liquid crystals and macroscopic assembled fibres. *Nat. Commun.* 2011, 2. DOI: 10.1038/ncomms1583

[21] Z. Xu, H. Sun, X. Zhao, C. Gao. *Adv. Mater.* 2013, 25, 188-193.

[22] R. Jalili, S. H. Aboutalebi, D. Esrafilzadeh, R. L. Shepherd, J. Chen, S. Aminorroaya-Yamini, K. Konstantinov, A. I. Minett, J. M. Razal, G. G. Wallace. *Adv. Funct. Mater.* 2013, 23, 5345-5354.

[23] C. Huhu, D. Zelin, H. Chuangang, Z. Yang, H. Yue, Q. Liangti, C. Nan, D. Liming. *Nanoscale* 2013, 5, 3428-3434.

[24] X. Zhao, X. Lu, W. T. Y. Tze, P. Wang. *Biosens. Bioelectron.* 2010, 25, 2343-2350.

[25] A. V. Neimark, S. Ruetsch, K. G. Kornev, P. I. Ravikovitch. *Nano Lett.* 2003, 3, 419-423.

[26] L. Viet Thong, H. Kim, A. Ghosh, J. Kim, J. Chang, V. Quoc An, P. Duy Tho, J.-H. Lee, S.-W.

Kim, Y. H. Lee. *ACS Nano* 2013, 7, 5940-5947.
[27] X. Chen, L. Qiu, J. Ren, G. Guan, H. Lin, Z. Zhang, P. Chen, Y. Wang, H. Peng. *Adv. Mater.* 2013, 25, 6436-6441.
[28] K. Wang, Q. Meng, Y. Zhang, Z. Wei, M. Miao. *Adv. Mater.* 2013, 25, 1494-1498.
[29] J. A. Lee, M. K. Shin, S. H. Kim, H. U. Cho, G. M. Spinks, G. G. Wallace, M. D. Lima, X. Lepro, M. E. Kozlov, R. H. Baughman *et al. Nat. Commun.* 2013, 4.DOI: 10.1038/ncomms2970
[30] Y. Li, K. Sheng, W. Yuan, G. Shi. *Chem. Commun.* 2013, 49, 291-293.
[31] Y. Fu, X. Cai, H. Wu, Z. Lv, S. Hou, M. Peng, X. Yu, D. Zou. *Adv. Mater.* 2012, 24, 5713-5718.
[32] X. Xiao, T. Li, P. Yang, Y. Gao, H. Jin, W. Ni, W. Zhan, X. Zhang, Y. Cao, J. Zhong *et al. ACS Nano* 2012, 6, 9200-9206.
[33] J. Bae, M. K. Song, Y. J. Park, J. M. Kim, M. Liu, Z. L. Wang. *Angew. Chem.Int. Ed.* 2011, 50, 1683-1687.
[34] Y. Fu, H. Wu, S. Ye, X. Cai, X. Yu, S. Hou, H. Kafafy, D. Zou. *Energy Environ. Sci.* 2013, 6, 805-812.
[35] W. Zhou, K. Zhou, X. Liu, R. Hu, H. Liu, S. Chen. *J. Mater. Chem. A* 2014, 2, 7250-7255.
[36] D. Zhang, M. Miao, H. Niu, Z. Wei. *ACS Nano* 2014, 8, 4571-4579.
[37] Y. Gogotsi & P. Simon. *Science* 2011, 334, 917-918.

**Figure captions**

Figure 1. The wet spinning apparatus for the synthesis of continuous neat graphene fibers and the processing steps for the assembly of flexible solid-state micro-SCs.

Figure 2. Photographs of the as-prepared neat graphene fibers collected in coagulation bath (a), SGFs being bent into different shapes to make up a number of "1952" and a word of "SCUT" (b), a blue light emission diode lamp connected to a power supply by two SGFs with the length of 2 cm as conducting wires (c); Comparison of electrical conductivities of the GO fibers before reduction (SGOFs) and after reduction (SGFs) (d). Scale bar: 1cm (c).

Figure 3. A photograph of a metal needle (a); SEM images of the inwall of the needle (b,c), a SGF electrode (d-f), and the inwall of a PTFE tube (g,h) and a PGF electrode (i). Scale bars: 2mm(a), 10 μm(c), 50 μm(d), 10 μm(e), 300 nm(f), 200μm(g), 40 μm (h), 2 μm (i).

Figure 4. CV curves of the micro-SCs based on SGFs and PGFs obtained at a scan rate of 50 $mV \cdot s^{-1}$ (a), and the micro-SCs based on SGFs at different scan rates varied from 2 to 10 $mV \cdot s^{-1}$ (b); CC curves of the micro-SCs based on SGFs obtained at different current densities varied from 0.12 to 0.32 $mA \cdot cm^{-2}$ (c); The areal specific capacitance of a SGFs' electrode (d).

Figure 5. Cycling stability of a micro-SC based on SGFs over 10000 cycles at a current density of 0.2 $mA \cdot cm^{-2}$, with the CC curves of the corresponding micro-SC in the inset (a); CV curves for a micro-SC based on SGFs in different conditions, with the corresponding digital image in the inset (b); Areal (c) and Volumetric (d) Ragone

plots to compare the micro-SCs based on SGFs with the previously reported devices. The Ragone plots for pen ink supercapacitors and all-graphene core sheath graphene fiber supercapacitors were obtained from ref. [31] and ref. [18], respectively. Data for RGO+CNT yarn supercapacitors, the lithium battery, 5.5V/100mF commercial supercapacitor and Al electrolytic supercapacitors were from ref. [7]. Besides, the Ragone plots for the biscrolled supercapacitors are from ref. [29].

Figure 6. A photograph of the three micro-SCs connected in series (a); CC curves of the corresponding device shown in “photograph (a)” (b); a photograph of the three micro-SCs connected in parallel (c); CC curves of the corresponding device shown in “photograph (c)” (d); photographs of the micro-SCs based on SGFs before being charge (e) and after being charged (f).

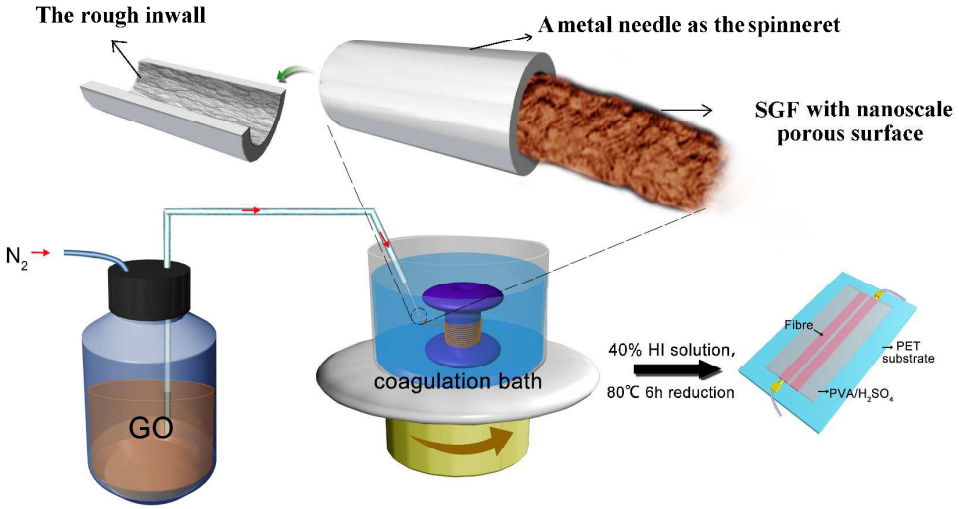


A metal needle spinneret was found to be the key component to synthesize neat graphene fibers with porous surface in the wet spinning process. The as-prepared neat graphene fibers possessing an impressive specific surface area up to 839 $m^2 \cdot g^{-1}$ and an excellent specific capacitance of 228 $mF \cdot cm^{-2}$ at 39.7 $\mu A \cdot cm^{-2}$ could be further assembled into solid-state micro-supercapacitors (micro-SCs) by following the processing steps. The micro-SCs displayed remarkable energy densities (7.9 $\mu Wh \cdot cm^{-2}$ or 4.0 $mWh \cdot cm^{-3}$) approaching those of thin-film lithium batteries.

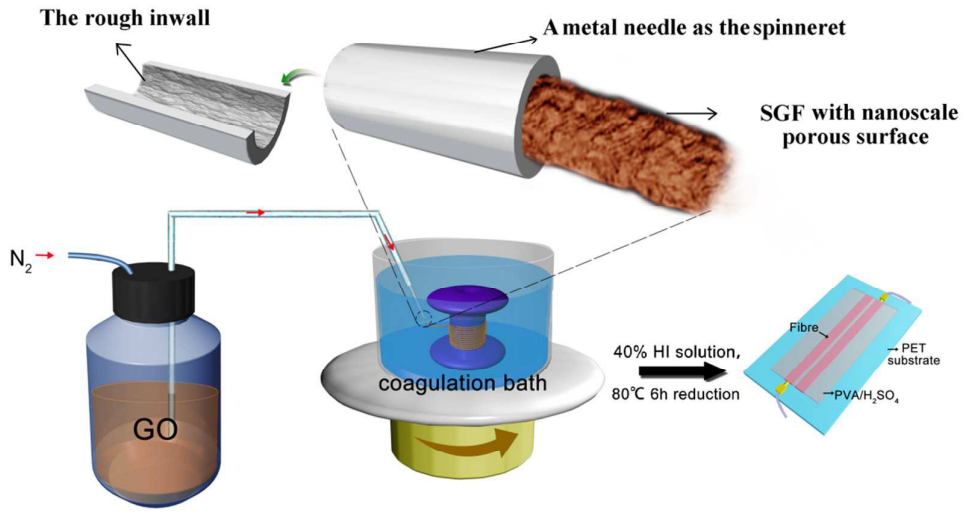


**Figure 1**

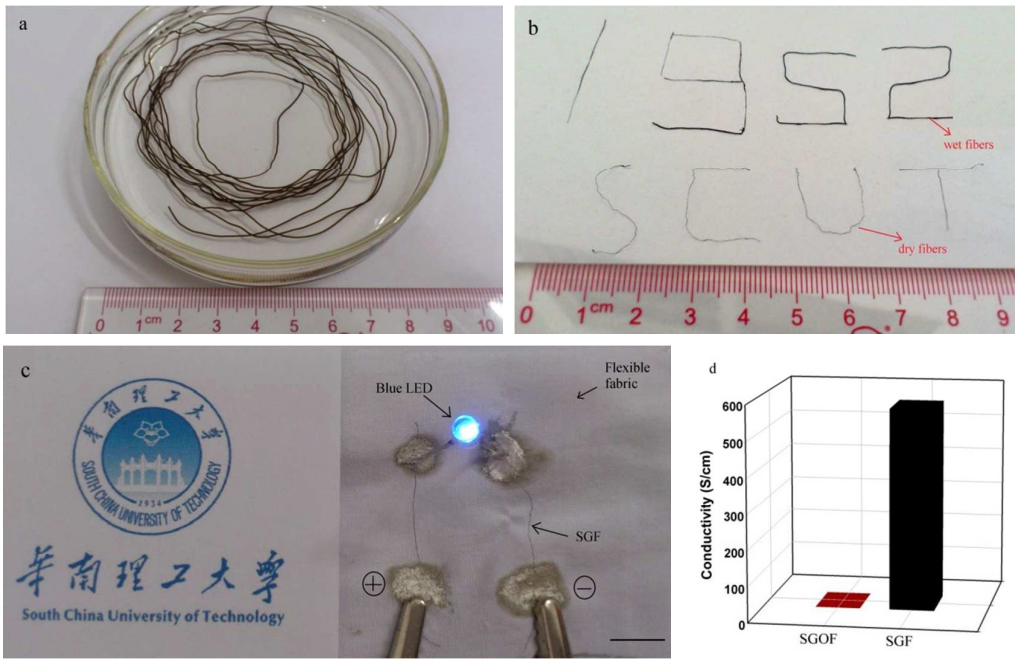


**Figure 2**

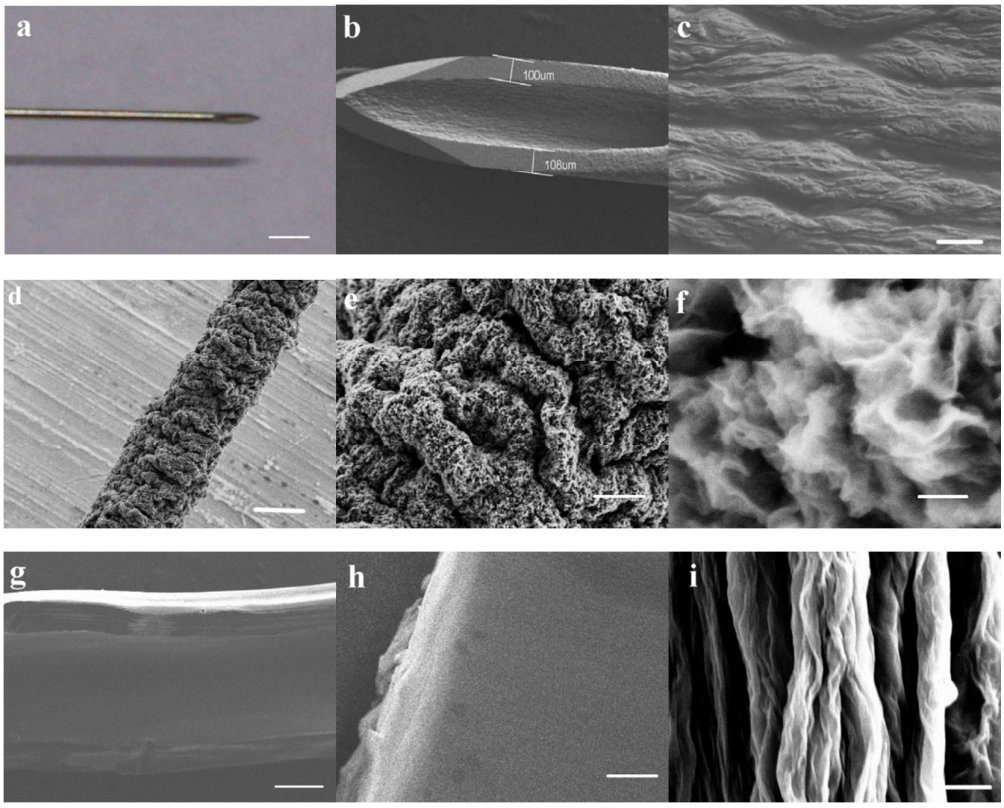


**Figure 3**

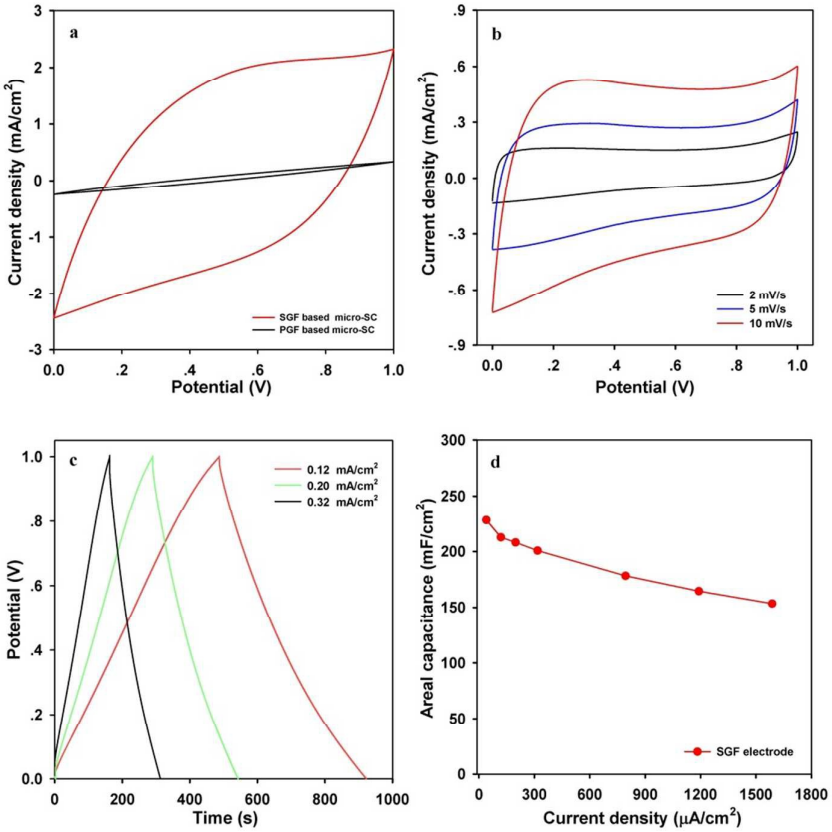


**Figure 4**

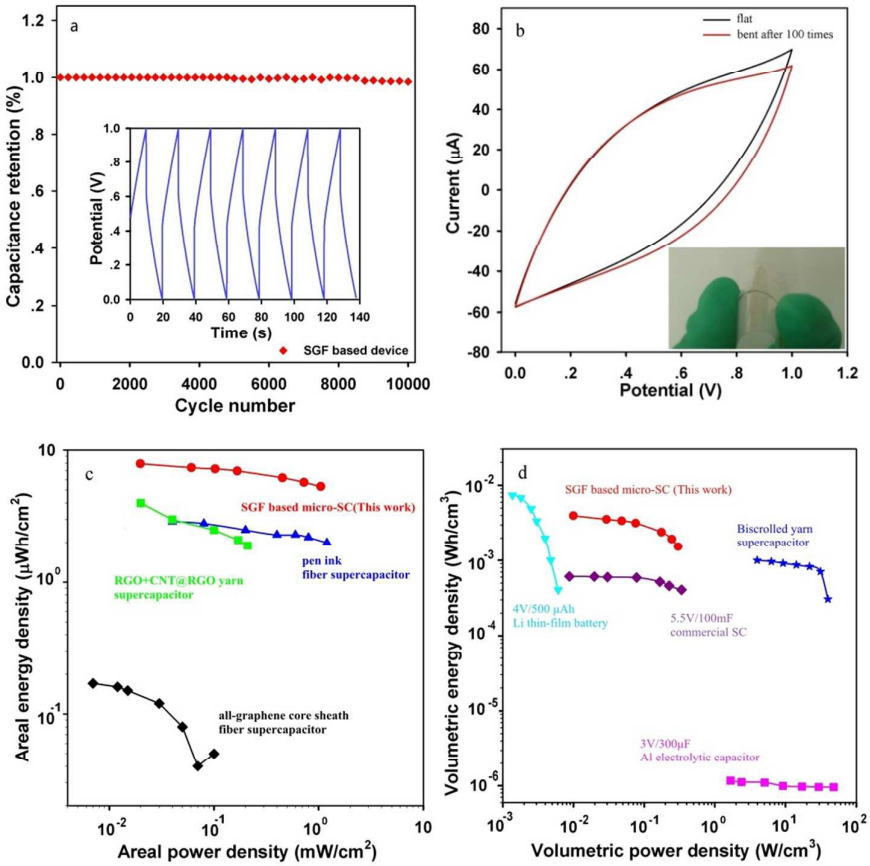


**Figure 5**

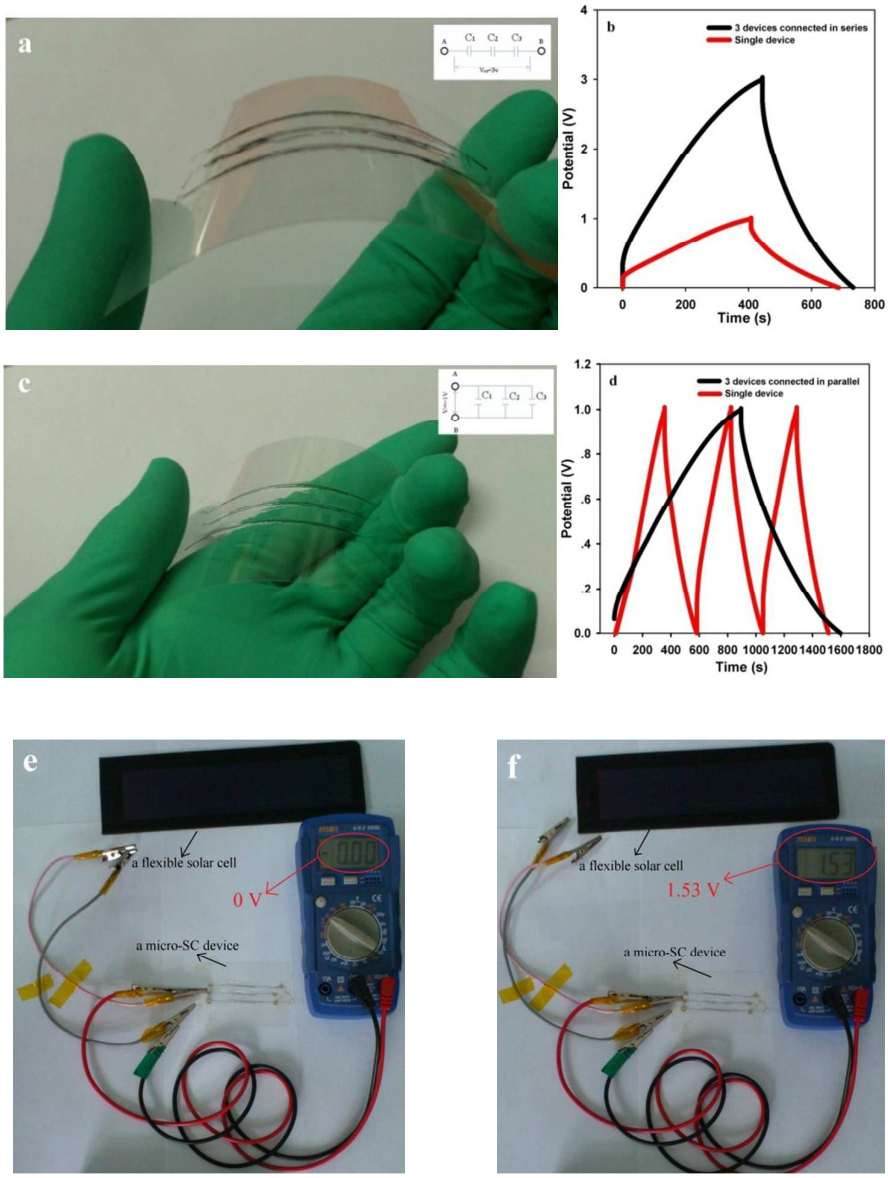


**Figure 6**